(12) INTERNATIONAL APPLICATION PUBLISHED UNDER THE PATENT COOPERATION TREATY (PCT)

(19) World Intellectual Property Organization
International Bureau

(43) International Publication Date
27 October 2016 (27.10.2016)

WIPO | PCT

(10) International Publication Number
WO 2016/170539 A1

(51) International Patent Classification:
G01R 33/00 (2006.01) *H01L 39/22* (2006.01)
G01R 33/02 (2006.01) *H01L 39/14* (2006.01)

(21) International Application Number:
PCT/IL2016/050421

(22) International Filing Date:
20 April 2016 (20.04.2016)

(25) Filing Language: English

(26) Publication Language: English

(30) Priority Data:
62/149,671 20 April 2015 (20.04.2015) US

(71) Applicant: **YEDA RESEARCH AND DEVELOPMENT CO. LTD.** [IL/IL]; at The Weizmann Institute of Science, P.O. Box 95, 7610002 Rehovot (IL).

(72) Inventors: **ZELDOV, Eli**; 16 Clil Street, 7630968 Rehovot (IL). **URI, Aviram**; c/o Yeda Research and Development Co. Ltd., at the Weizmann Institute of Science, P.O. Box 95, 7610002 Rehovot (IL). **ANAHORY, Yonathan**; c/o Yeda Research and Development Co. Ltd., at the Weizmann Institute of Science, P.O. Box 95, 7610002 Rehovot (IL). **HOOVINAKATTE RANGANATH, Naren**; c/o Yeda Research and Development Co. Ltd., at the Weizmann Institute of Science, P.O. Box 95, 7610002 Rehovot (IL). **MAYASOEDOV, Yuri**; c/o Yeda Research and Development Co. Ltd., at the Weizmann Institute of Science, P.O. Box 95, 7610002 Rehovot (IL). **EMBON, Lior**; c/o Yeda Research and Development Co. Ltd., at the Weizmann Institute of Science, P.O. Box 95, 7610002 Rehovot (IL).

(74) Agents: **PEARL COHEN ZEDEK LATZER BARATZ** et al.; P.o.box 12704, 4673339 Herzliya (IL).

(81) Designated States *(unless otherwise indicated, for every kind of national protection available)*: AE, AG, AL, AM, AO, AT, AU, AZ, BA, BB, BG, BH, BN, BR, BW, BY, BZ, CA, CH, CL, CN, CO, CR, CU, CZ, DE, DK, DM, DO, DZ, EC, EE, EG, ES, FI, GB, GD, GE, GH, GM, GT, HN, HR, HU, ID, IL, IN, IR, IS, JP, KE, KG, KN, KP, KR, KZ, LA, LC, LK, LR, LS, LU, LY, MA, MD, ME, MG, MK, MN, MW, MX, MY, MZ, NA, NG, NI, NO, NZ, OM, PA, PE, PG, PH, PL, PT, QA, RO, RS, RU, RW, SA, SC, SD, SE, SG, SK, SL, SM, ST, SV, SY, TH, TJ, TM, TN, TR, TT, TZ, UA, UG, US, UZ, VC, VN, ZA, ZM, ZW.

(84) Designated States *(unless otherwise indicated, for every kind of regional protection available)*: ARIPO (BW, GH, GM, KE, LR, LS, MW, MZ, NA, RW, SD, SL, ST, SZ, TZ, UG, ZM, ZW), Eurasian (AM, AZ, BY, KG, KZ, RU,

[Continued on next page]

(54) Title: ELECTRONICALLY-TUNABLE MULTI-JUNCTION MULTI-TERMINAL SQUID-ON-TIP

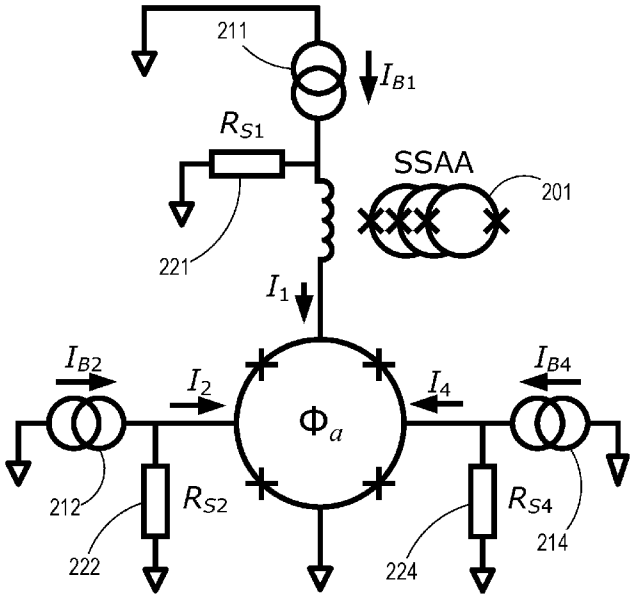


FIG. 2A

(57) Abstract: A nanoscale superconducting quantum interference device (SQUID) with an *in- situ* electronically tunable interference pattern. A four-terminal four-junction SQUID On Tip (mSOT) with effective diameter as small as 165 nm is fabricated at the apex of a sharp pipette using self-aligned three step deposition of Pb. In contrast to conventional two-junction two-terminal SQUIDs which display optimal sensitivity with an applied field biased to about quarter of flux quantum, ($\Phi_0/4$), the additional terminals and junctions allow attaining the optimal sensitivity at any value of the applied field, thus eliminating "blind spots". The device achieves spin sensitivity of 5 to 8 $\mu_B/Hz^{1/2}$ over a continuous field range of 0 to 0.5 T, thus providing a highly sensitive tool for high dynamic range nanoscale magnetic imaging.

WO 2016/170539 A1

TJ, TM), European (AL, AT, BE, BG, CH, CY, CZ, DE, DK, EE, ES, FI, FR, GB, GR, HR, HU, IE, IS, IT, LT, LU, LV, MC, MK, MT, NL, NO, PL, PT, RO, RS, SE, SI, SK, SM, TR), OAPI (BF, BJ, CF, CG, CI, CM, GA, GN, GQ, GW, KM, ML, MR, NE, SN, TD, TG).

Published:

— *with international search report (Art. 21(3))*

ELECTRONICALLY-TUNABLE MULTI-JUNCTION MULTI-TERMINAL SQUID-ON-TIP

CROSS REFERENCE TO RELATED APPLICATIONS

[001] This application claims priority of U.S. Provisional Patent Application Serial No. 62/149,671, filed April 20, 2015, entitled "Fabrication and characterization of multi-junction, multi-terminal Superconducting Quantum Interference Device On a Tip", which is incorporated in its entirety herein by reference.

BACKGROUND

[002] In recent years there has been growing interest in the development of nanoscale magnetic characterization tools in order to address the rapidly evolving fields of nanomagnetism and spintronics.

[003] Scanning micro and nanoscale superconducting quantum interference devices (SQUIDs) are of particular interest in magnetic imaging, because of their high-sensitivity and high bandwidth. The two main technological approaches for the fabrication of scanning SQUIDs are based on planar lithographic methods and on self-aligned SQUID-on-tip (SOT) deposition.

[004] Planar SQUIDs have the benefit of robust structure and the possible integration of pickup and modulation coils that allow operation of the SQUID at its highest sensitivity flux bias conditions using a flux-locked loop (FLL) feedback mechanism.

[005] The SOT, on the other hand, has the advantage of very small size, nanoscale proximity to the sample, and operation at high fields. The inability to use an FLL, however, poses a significant drawback as the high sensitivity of the SOT is achieved

only at specific field values leaving substantial intermediate field regions as "blind spots".

[006] In conventional SQUID setups the magnetic field of the sample is not coupled to the SQUID loop directly but rather through a pickup coil. As a result, by adding a modulation coil or an integrated current-carrying element, the total flux in the SQUID loop can be maintained at its optimal bias while the sample can be exposed to any value of the applied magnetic field. The nanoscale proximity of the SOT to the sample surface, which is its key advantage, however, dictates that *the flux in the SQUID loop cannot be varied without a corresponding invasive change in the local field of the sample*. As a result, *the FLL configuration cannot be used in direct nanoscale magnetic imaging*.

SUMMARY

[007] Various embodiments of the present invention provide a novel multi-terminal multi-junction SQUID-On-Tip (mSOT) that allows sensitive continuous operation over a wide range of fields with spin sensitivity better than 8 $\mu_B/Hz^{1/2}$. In contrast to the FLL used in conventional SQUIDs, embodiments of the present invention feature a *superconducting phase locked loop* (SPLL) that allows *in-situ* electronic control of the SQUID's quantum interference pattern without the need to modify the flux in the SQUID loop. As a result, nanoscale magnetic imaging can be performed with optimal sensitivity at any value of the local field without "blind spots" and without affecting the local field. According to these embodiments, driving a current through a control terminal modifies the superconducting phase across one of the junctions, thus shifting the quantum interference pattern. A single control terminal allows shifting the pattern by

half a period while two terminals enable a shift by a full period. As a result, various additional noise reduction schemes can be implemented analogous to the ones based on FLL protocols. An mSOT according to certain embodiments of the invention thus provide a new electronically-tunable tool for highly sensitive quantitative imaging and study of nanoscale magnetic phenomena over a large dynamic range.

[008] In particular, these embodiments provide a feedback mechanism that is advantageous to a variety of SQUIDs but is of crucial importance to SOTs. According to these embodiments, instead of controlling the magnetic flux in the SQUID loop, the phase of the superconducting order parameter in the loop is *in-situ* controlled. The resulting SPLL provides highly sensitive noninvasive SQUID operation at any value of the applied magnetic field.

[009] The basic principle of SPLL operation can be understood by considering an ideal SQUID with no inductance in its superconducting state,, which is described by:

$$\varphi_1 + \varphi_2 + 2\pi(\Phi_a/\Phi_0) = 2\pi n \qquad \text{(Equation 1)}$$

[0010] where φ_i is the superconducting phase difference across each of the Josephson junctions (JJ), Φ_a is the applied flux in the loop, Φ_0 is the flux quantum, and n is an integer. In the following we consider the situation of $n = 0$ for simplicity. The highest sensitivity of the SQUID is achieved when $\varphi_1 + \varphi_2 \approx \pi/2$ corresponding to an applied flux of $|\Phi_a| \approx \Phi_0/4$. Since, at the critical current, φ_1 and φ_2 also have to satisfy the requirement of maximum total supercurrent through the SQUID, there are no free degrees of freedom and the phases φ_1 and φ_2 of the two junctions at the critical current conditions are uniquely defined. Hence operation at the optimal sensitivity can be achieved only if the FLL maintains the net flux in the SQUID loop at $|\Phi_a| \approx \Phi_0/4$.

[0011] Therefore, according to an embodiment of the present invention, there is provided a multi-terminal multi-junction Superconducting Quantum Interference Device On Tip (mSOT) apparatus including: (a) a multi-terminal multi-junction Superconducting Quantum Interference Device On Tip including: (b) a superconducting loop with a first Josephson Junction, a second Josephson Junction, and a third Josephson Junction; (c) a first terminal electrically connected to the loop between the third Josephson Junction and the first Josephson Junction; (d) a second terminal electrically connected to the loop between the first Josephson Junction and the second Josephson Junction; and (e) a third terminal electrically connected to the loop between the second Josephson Junction and the third Josephson Junction; and (f) a bias current source for applying a bias current to the first terminal; and (g) a first control current source for applying a first control current to the second terminal.

[0012] In addition, according to another embodiment of the present invention, there is also provided a method for operating a multi-terminal multi-junction Superconducting Quantum Interference Device On Tip (mSOT) which includes: (a) a superconducting loop with a first Josephson Junction, a second Josephson Junction, and a third Josephson Junction; (b) a first terminal electrically connected to the loop between the third Josephson Junction and the first Josephson Junction; (c) a second terminal electrically connected to the loop between the first Josephson Junction and the second Josephson Junction; and (d) a third terminal electrically connected to the loop between the second Josephson Junction and the third Josephson Junction; (e) wherein the mSOT has a current-flux response function, and wherein the current-flux response function has a maximum absolute value; the method including: (f) applying a bias current to the first terminal; (g) applying a first control current through the second terminal; (h) and

adjusting the first control current to minimize a flux noise of the mSOT for a given applied magnetic field.

BRIEF DESCRIPTION OF THE DRAWINGS

[0013] The subject matter disclosed may best be understood by reference to the following detailed description when read with the accompanying drawings in which:

[0014] Fig. 1A is a schematic diagram of an mSOT showing a SQUID loop with four junctions and four terminals, according to an embodiment of the present invention.

[0015] Fig. 1B illustrates a cross section of the quartz tube with its four grooves and Pb film formed by two side depositions, according to an embodiment of the present invention.

[0016] Fig. 1C is a side-view scanning electron micrograph of a device according to an embodiment of the present invention.

[0017] Fig. 1D is a top view scanning electron micrograph of the device shown in Fig. 1C.

[0018] Fig. 2A is a schematic diagram of an mSOT electrical circuit according to an embodiment of the present invention.

[0019] Fig. 2B illustrates mSOT electrical characteristics at various values of B_a, acquired at I_{B2} = 74 μA and I_{B4} = 0.

[0020] Fig. 2C illustrates current noise spectral density $S_I^{1/2}$ and corresponding flux noise $S_\Phi^{1/2}$ at B_a = 0.2 T at the optimal working point.

[0021] Fig. 3A illustrates an interference pattern $I_{c1}(B_a)$ at three values of control current I_{B2} = -150, -30, and 90 μA at $I_{B4} = 0$, according to an embodiment of the invention.

[0022] Fig. 3B is a plot of $I_{c1}(I_{B2}, B_a)$ showing a continuous shift of the interference pattern with the control current I_{B2} at $I_{B4} = 0$.

[0023] Fig. 3C – Fig. 3E illustrate an mSOT current-flux response function, $dI_1/d\Phi_a$, for three values of I_{B2} at $I_{B4} = 0$ showing the shift in field of the sensitive regions as the control current is varied.

[0024] Fig. 4 is a plot of flux noise and spin noise in an mSOT device according to an embodiment of the present invention, comparing the noise levels of the device with and without application of SPLL.

[0025] Fig. 5 is a flowchart illustrating a method according to an embodiment of the present invention.

[0026] Fig. 6 is a flowchart illustrating another method according to a related embodiment of the present invention.

[0027] Fig. 7 is a flowchart illustrating a further method according to another related embodiment of the present invention.

[0028] For simplicity and clarity of illustration, elements shown in the figures are not necessarily drawn to scale, and the dimensions of some elements may be exaggerated relative to other elements. In addition, reference numerals may be repeated among the figures to indicate corresponding or analogous elements.

DETAILED DESCRIPTION

[0029] SPLL operation is based incorporating additional degrees of freedom by integrating additional junctions and terminals in the SQUID loop as shown schematically in Fig. 1A. According to certain embodiments of the present invention, there are at least three junctions and the number of terminals is equal to the number of junctions; *i.e.*, every superconducting segment bordered by adjacent junctions is connected to its own terminal. In other embodiments, however, there are at least four junctions and at least three terminals, but not every segment has its own terminal.

[0030] Multi-junction configurations as well as multi terminal ones have been used in the past for logical circuits, enhanced SQUID capabilities, variable inductances, and flux modulation. In contrast, embodiments of the present invention use the additional degrees of freedom for phase control, rather than flux control, of the quantum interference pattern of the SQUID.

[0031] Fig. 1A shows a schematic configuration of an mSOT according to an embodiment of the invention. A superconducting loop **100** provides a circuit for current flow around an area **110** through which passes a magnetic flux Φ_a. A current I_1 is applied to a first terminal **101** ("terminal 1"). A third terminal **103** ("terminal 3") functions as a current drain to ground, such that $I_3 = I_1 + I_2 + I_4$. A second terminal **102** ("terminal 2") and a fourth terminal **104** ("terminal 4") are used to provide control currents I_2 and I_4, respectively. Loop **100** has four identical Josephson junctions: a first junction **111**, a second junction **112**, a third junction **113**, and a fourth junction **114**, through which currents J_1, J_2, J_3, and J_4 circulate as indicated. For this structure Equation 1 is replaced by:

$$\varphi_1 + \varphi_2 + \varphi_3 + \varphi_4 + 2\pi(\Phi_a/\Phi_0) = 2\pi n \quad \text{(Equation 2)}$$

[0032] In a similar fashion to the case of a two-junction SQUID, the most sensitive SQUID response in the absence of control currents is achieved when $\varphi_1 + \varphi_2 + \varphi_3 + \varphi_4 \approx \pi/2$. The condition $I_2 = I_4 = 0$ dictates that $\varphi_1 = \varphi_2$ and $\varphi_3 = \varphi_4$, and hence $\varphi_1 + \varphi_4 = \varphi_2 + \varphi_3 \approx \pi/4$, restricting the optimal sensitivity operation to $|\Phi_a| \approx \Phi_0/4$ as in the case of a regular SQUID. However, by allowing control currents to flow through terminal 2 (**102**) and terminal 4 (**104**), this restriction is lifted as follows:

[0033] In the absence of control currents, the critical current $I_{c1}(\Phi_a)$ reaches its maximum value of $I_{c1}^{max} = 2J_0$ at zero applied flux $\Phi_a = 0$ where first junction **111** and fourth junction **114** each carry maximal dissipationless current J_0, inducing a phase drop of $\varphi_1 = -\varphi_4 = \pi/2$. For simplicity current I_4 is fixed at $I_4 = 0$, thus imposing the condition that $\varphi_3 = -\varphi_4$, while the control current I_2 is given by $I_2 = J_2 - J_1 = J_0(\sin\varphi_2 - \sin\varphi_1) = J_0(\sin\varphi_2 - 1)$. For any applied flux Φ_a, $\varphi_1 = -\varphi_4 = -\varphi_3 = \pi/2$ is kept fixed and φ_2 is modified by adjusting I_2 to satisfy Equation 2. Since φ_1 and φ_4 are not changed, the current I_1 of the mSOT remains at its maximal critical value as previously specified, namely $I_{c1}(\Phi_a, I_2) = I_{c1}(0, 0) = I_{c1}^{max} = 2J_0$, where the control current I_2 required to keep I_{c1} at its maximum is given by Equation 3:

$$I_2 = J_0(\sin\varphi_2 - 1) = J_0(\sin(\pi/2 - 2\pi\Phi_a/\Phi_0) - 1)$$

$$= J_0(\cos(2\pi\Phi_a/\Phi_0) - 1) \quad \text{(Equation 3)}$$

[0034] Thus, according to various embodiments of the present invention the quantum interference pattern $I_{c1}(\Phi_a)$ of the mSOT is shifted as a whole via electronic means by

applying control currents I_2 and I_4. In particular, according to embodiments of the present invention, for any value of the applied flux Φ_a a control current exists that biases the mSOT to the most sensitive working point. According to a related embodiment, this control is applicable to any SQUID with at least three junctions and three terminals including asymmetric junctions, non-sinusoidal current-phase relations, and the presence of finite inductance. In contrast to the previously-known FLL, by which the interference pattern is shifted by applying additional flux to the SQUID loop, SPLL embodiments of the present invention, as disclosed herein, achieve a shift of the pattern by controlling the superconducting phase across one (or more) additional junctions in the loop. As a result, a very sensitive measurement of the local magnetic field of a sample can be attained at any value of the local field thus eliminating the "blind spots". Note also, that due to its very small size the geometrical inductance of the SOT is several orders of magnitude smaller than its kinetic inductance. As a result, the control current affects the superconducting phase across the junctions with negligible change to the self-induced flux in the SQUID loop.

[0035] A two-terminal SOT may be fabricated by self-aligned two-sided deposition of two superconducting leads along a pulled quartz pipette followed by a third deposition on the apex ring. The principal challenge in fabricating the mSOT is in attaining nanoscale multi-terminal connections to the apex.

[0036] According to particular embodiments of the invention, fabrication of an mSOT begins with a quartz tube or pipette having an outer diameter of the order of 1 mm, and having four 0.1×0.15 mm^2 grooves equally spaced on its outer circumference, which maintain their relative shape upon laser heating and pulling, and which extend to an

apex formed during the pulling. Fig. 1B illustrates a cross-section of the finished mSOT according to a related embodiment of the present invention, and Figs. 1C and 1D are scanning electron microscope (SEM) images of the mSOT exterior and tip. The grooves provide shading during two side depositions of lead (Pb) to create four gaps **171**, **172**, **173**, and **174**, respectively associated with the grooves, and separating four leads **153**, **154**, **155**, and **156**. One side Pb deposition is made in a direction **161**, and the other side deposition is made in a direction **162**. Quartz body **151** has a hollow interior **152** which extends the full length of the mSOT to an apex ring **181**. In a third Pb deposition on apex ring **181**, four constrictions are formed in the regions of gaps **171**, **172**, **173**, and **174**, creating Dayem-bridge weak links to establish a self-aligned four-junction four-terminal mSOT. Other embodiments of the invention utilize other superconducting materials, non-limiting examples of which include Indium (In), Niobium (Nb), and combinations of different materials, such as Pb-In. Still further embodiments of the invention provide other fabrication techniques, such as lithographic techniques, for producing mSOTs.

[0037] According to a related embodiment, an mSOT is characterized at 4.2 K using the electrical circuit shown in Fig. 2A, where a current bias I_{B1} from a current source **211** is applied to the mSOT in parallel with a shunt resistor **221** (R_{S1}). The resulting current I_1 flowing into the mSOT is measured using a series SQUID array amplifier (SSAA) **201**. The control currents I_2 and I_4 are provided by applying to the mSOT control bias currents I_{B2} from a current source **212** and I_{B4} from a current source **214**, respectively, in parallel with a shunt resistor **222** and a shunt resistor **224**, respectively. In a related embodiment, the control terminals of the mSOT are current biased, and thus shunt

resistors **222** and **224** are unnecessary. Fig. 2B illustrates electrical characteristics $I_1(I_{B1})$ of the mSOT device showing the measured I_1 versus the applied bias current I_{B1} at several values of the applied field B_a. For $I_1 < I_{c1}(B_a)$ the mSOT is in the superconducting state and most of the applied current I_{B1} flows through the device. When I_1 reaches $I_{c1}(B_a)$ the mSOT becomes resistive and a significant part of the current is diverted to shunt resistor **201** R_{S1}. At higher biases a number of resonances are visible.

[0038] To illustrate the electronic tunability of an mSOT according to an embodiment of the present invention, Fig. 3A shows an interference pattern of the critical current $I_{c1}(B_a)$ derived from electrical characteristics, in a curve **301** for I_{B2} = 90 μA, a curve **302** for I_{B2} = -30 μA, and a curve **303** for I_{B2} = -150 μA. An interference period **304** of 97 mT corresponding to an effective loop diameter of 165 nm agrees with the dimensions shown in the SEM image of Fig. 1D. According to embodiments of the present invention, a noteworthy feature illustrated by Fig. 3A is the *in-situ* electronic tunability of the mSOT. The three presented $I_{c1}(B_a)$ curves **301**, **302**, and **303** show that the entire pattern is readily shifted horizontally by varying the control bias current I_{B2} (keeping $I_{B4} = 0$ for simplicity). Fig. 3B shows that the critical current interference pattern $I_{c1}(B_a, I_{B2})$ is shifted continuously with I_{B2} over a large span of about half a period between the lowest and highest presented values of I_{B2}. This implies that for any value of B_a there is a current I_{B2} for which maximum mSOT sensitivity can be attained at this field, thus allowing optimal operation at any B_a without “blind spots”.

[0039] The first two terms of Equation 3 can be rewritten as $I_2(B_a) = J_2(\varphi_2) - J_0$, namely curves **305**, **306**, and **307** tracing the maximum critical current I_{c1}^{max} in Fig. 3B depict the current-phase relation $J_2(\varphi_2)$ of junction 2. This correspondence holds for any form of current-phase relations and therefore provides a general tool for direct probing of current-phase relations in various systems.

[0040] Achieving highly sensitive continuous operation with low flux noise $S_\Phi^{1/2} = S_I^{1/2}/|dI_1/d\Phi_a|$ requires a high response (*i.e.*, derivative of current with respect to flux $|dI_1/d\Phi_a|$) and a low current noise $S_I^{1/2}$ at all values of the applied field. Fig. 3C shows the measured current-flux response function $dI_1/d\Phi_a$ versus bias current I_{B1} and the applied field B_a for a bias current of $I_{B2} = 90$ μA. The blue and red regions have high values of $|dI_1/d\Phi_a|$ whereas the green regions have no sensitivity due to either the condition that $I_1 < I_{c1}(B_a)$, or are "blind spots" where $dI_1/d\Phi_a \approx 0$. According to embodiments of the present invention, varying I_{B2} shifts the sensitive regions to the desired value of B_a as shown in Figs. 3D and 3E.

[0041] A spectrum of the current noise $S_I^{1/2}$ of the mSOT is shown in Fig. 2C, displaying a $1/f$ behavior at low frequencies $f \lesssim 1$ kHz followed by white noise at higher frequencies.

[0042] By measuring the white noise level and the current-flux response function $dI_1/d\Phi_a$, the flux noise $S_\Phi^{1/2} = S_I^{1/2}/|dI_1/d\Phi_a|$ of the mSOT versus B_a is derived. The spin noise $S_n^{1/2}$ in units of $\mu_B/\mathrm{Hz}^{1/2}$ is related to the flux noise through $S_n^{1/2} = S_\Phi^{1/2} r/r_e$, where $S_\Phi^{1/2}$ is in units of $\Phi_0/\mathrm{Hz}^{1/2}$; $r_e = 2.82 \times 10^{-15}$ m is the

classical electron radius; and $r = 82$ nm is the effective radius of the mSOT. To minimize the noise, the absolute value of the current-flux response function $|dI_1/d\Phi_a|$ is maximized. Absolute value is taken, because only the magnitude of the quantity is significant – the sign does not matter. In descriptions herein of embodiments of the present invention, the term "*current-flux response function*" denotes the absolute value $|dI_1/d\Phi_a|$.

[0043] Fig. 4 shows both flux noise (left axis) and spin noise (right axis) of an mSOT device. A curve **401** with units on the left axis displays the flux noise measured at $I_{B2} = I_{B4} = 0$ (*i.e.*, no control current), reflecting conventional two-terminal SOT operation. Curve **401** shows high noise levels in the "blind spot" regions – the large peaks in the flux noise of curve **401** correspond to regions where $|dI_1/d\Phi_a|$ is small.

[0044] In contrast, a curve **402** shows the performance of the same mSOT device operating in the SPLL mode by adjusting the control currents according to embodiments of the present invention. For each value of B_a, optimal values of the control currents I_{B2} and I_{B4} are determined, which bias the mSOT to its optimal working point and thereby minimize the flux noise. The additional degrees of freedom provided by the control currents result in the elimination of "blind spots" and a uniform and low noise of 5 to 8 $\mu_B/\mathrm{Hz}^{1/2}$ over a previously unattainable continuous range of applied fields from 0 to 0.5 T.

[0045] In various embodiments of the present invention, therefore, the performance of the mSOT is optimized by minimizing the flux noise $S_\Phi^{1/2}$ for a given magnetic field. In a particular embodiment, this is done by minimizing the current noise $S_I^{1/2}$ as well as

maximizing the current-flux response function $|dI_1/d\Phi_a|$; in a related embodiment, the current noise $S_I^{1/2}$ is determined by other considerations, and only the current-flux response function $|dI_1/d\Phi_a|$ is maximized for a given magnetic field.

[0046] For the following methods, an mSOT characterization measurement of the current through terminal **101** (terminal 1) $I_1(B_a, I_{B1}, I_{B2}, I_{B4})$ is performed. From this, derive $S_\Phi^{1/2}(B_a, I_{B1}, I_{B2}, I_{B4})$. Then magnetic field B_a may be inferred from bias current I_1 and control currents I_{B1}, I_{B2}, and I_{B4} by adjusting them to obtain optimal flux noise levels for B_a.

[0047] Fig. 5 is a flowchart illustrating a method according to an embodiment of the present invention for operating an mSOT **500** having three terminals **501**, **502**, and **503**; and three junctions **511**, **512**, and **513**. In a step **521** a bias current I_1 is applied through terminal **501**, and in a step **522** a value of current-flux response function $|dI_1/d\Phi_a|$ is obtained. Next, in a step **523**, a control current I_2 is applied through terminal **502**. In a step **524** a maximum value of the current-flux response function, $|dI_1/d\Phi_a|^{max}$, is obtained. Finally, in a step **525**, control current I_2 is adjusted to maximize the current-flux response function $|dI_1/d\Phi_a|$, so that $|dI_1/d\Phi_a|$ is substantially at the maximum value $|dI_1/d\Phi_a|^{max}$ (*i.e.*, so that $|dI_1/d\Phi_a| \cong |dI_1/d\Phi_a|^{max}$).

[0048] Fig. 6 is a flowchart illustrating another method according to a related embodiment of the present invention for operating an mSOT **600** having four terminals **601**, **602**, **603**, and **604**; and four junctions **611**, **612**, **613**, and **614**. In a step **621** a bias current I_1 is applied through terminal **601**, and in a step **622** a value of current-flux response function $|dI_1/d\Phi_a|$ is obtained. Next, in a step **623**, a first control current I_2 is

applied through terminal **602**. In a step **624** a second control current I_4 is applied through terminal **604**. Then, in a step **625**, a maximum value of the current-flux response function, $|dI_1/d\Phi_a|^{max}$, is obtained. Finally, in a step **626**, first control current I_2 and second control current I_4 are adjusted to maximize the current-flux response function $|dI_1/d\Phi_a|$, so that $|dI_1/d\Phi_a|$ is substantially at the maximum value $|dI_1/d\Phi_a|^{max}$ (*i.e.*, so that $|dI_1/d\Phi_a| \cong |dI_1/d\Phi_a|^{max}$).

[0049] Fig. 7 illustrates a further method according to another related embodiment of the present invention, which can be carried out to augment the methods disclosed above. In a step **701**, the mSOT is characterized according to measurements of the current $I_1(B_a, I_{B1}, I_{B2}, I_{B4})$ and the current noise $S_I^{1/2}(B_a, I_{B1}, I_{B2}, I_{B4})$ as described previously, to obtain a flux noise characterization **711** $S_\Phi^{1/2} = S_I^{1/2}/|dI_1/d\Phi_a|$. Next, in a step **702**, a set **712** of mSOT working regions is obtained. A working region is specified by a rough value of I_1 for mSOT operation. Then, in a step **703** the bias of the mSOT is adjusted for a working region selected from set **712**. In a related embodiment, the selection of working region is arbitrary. Following this, in a step **704** I_1 is measured and an estimated value **713**, B_a^{est}, is inferred from the measurement of I_1 according to characterization **711**. Because value **713** is only an estimate, in a step **705**, the mSOT is fine-tuned to an optimal working point of minimal noise. Finally, in a step **706** I_1 for the optimal working point is measured, and a measured value **714**, B_a^{meas}, is inferred from the measurement of I_1 according to characterization **711**.

CLAIMS

What is claimed is:

1. A multi-terminal multi-junction Superconducting Quantum Interference Device On Tip (mSOT) apparatus comprising:

a multi-terminal multi-junction Superconducting Quantum Interference Device On Tip comprising:

a superconducting loop with a first Josephson Junction, a second Josephson Junction, and a third Josephson Junction;

a first terminal electrically connected to the loop between the third Josephson Junction and the first Josephson Junction;

a second terminal electrically connected to the loop between the first Josephson Junction and the second Josephson Junction; and

a third terminal electrically connected to the loop between the second Josephson Junction and the third Josephson Junction; and

a bias current source for applying a bias current to the first terminal; and

a first control current source for applying a first control current to the second terminal.

2. The multi-terminal multi-junction Superconducting Quantum Interference Device On Tip (mSOT) apparatus of claim 1, further comprising:

a fourth Josephson Junction between the third Josephson Junction and the first Josephson Junction;

a fourth terminal electrically connected to the loop between the third Josephson Junction and the fourth Josephson Junction,

wherein the third terminal is electrically connected to the loop between the second Josephson Junction and the third Josephson Junction; and

a second control current source for applying a second control current to the fourth terminal.

3. The multi-terminal multi-junction Superconducting Quantum Interference Device On Tip (mSOT) apparatus of claim 1, wherein the superconducting loop is on the apex of a pulled pipette.

4. The multi-terminal multi-junction Superconducting Quantum Interference Device On Tip (mSOT) apparatus of claim 2, wherein the superconducting loop is on the apex of a pulled pipette.

5. The multi-terminal multi-junction Superconducting Quantum Interference Device On Tip (mSOT) apparatus of claim 3, wherein a Josephson Junction is a Dayem bridge weak link formed by a constriction in a region of a gap associated with a groove on the outer circumference of the pipette.

6. The multi-terminal multi-junction Superconducting Quantum Interference Device On Tip (mSOT) apparatus of claim 4, wherein a Josephson Junction is a Dayem bridge weak link formed by a constriction in a region of a gap associated with a groove on the outer circumference of the pipette.

7. The multi-terminal multi-junction Superconducting Quantum Interference Device On Tip (mSOT) apparatus of claim 1, wherein the first control current modifies the superconducting phase across a Josephson Junction.

8. The multi-terminal multi-junction Superconducting Quantum Interference Device On Tip (mSOT) apparatus of claim 2, wherein the first control current modifies the superconducting phase across a Josephson Junction and the second control current modifies the superconducting phase across a Josephson Junction.

9. The multi-terminal multi-junction Superconducting Quantum Interference Device On Tip (mSOT) apparatus of claim 7, wherein modifying the superconducting phase across a Josephson Junction shifts a quantum interference pattern.

10. The multi-terminal multi-junction Superconducting Quantum Interference Device On Tip (mSOT) apparatus of claim 8, wherein modifying the superconducting phase across a Josephson Junction shifts a quantum interference pattern.

11. A method for operating a multi-terminal multi-junction Superconducting Quantum Interference Device On Tip (mSOT) which includes:

a superconducting loop with a first Josephson Junction, a second Josephson Junction, and a third Josephson Junction;

a first terminal electrically connected to the loop between the third Josephson Junction and the first Josephson Junction;

a second terminal electrically connected to the loop between the first Josephson Junction and the second Josephson Junction; and

a third terminal electrically connected to the loop between the second Josephson Junction and the third Josephson Junction;

wherein the mSOT has a current-flux response function, and wherein the current-flux response function has a maximum absolute value;

the method comprising:

applying a bias current to the first terminal;

applying a first control current through the second terminal; and

adjusting the first control current to minimize a flux noise of the mSOT for a given applied magnetic field.

12. The method of claim 11, wherein to minimize the flux noise for the given applied magnetic field is accomplished by adjusting the first control current so that the current-flux response function is substantially equal to the maximum absolute value thereof.

13. The method of claim 11, wherein the multi-terminal multi-junction Superconducting Quantum Interference Device On Tip (mSOT) further includes:

a fourth Josephson Junction between the third Josephson Junction and the first Josephson Junction;

a fourth terminal electrically connected to the loop between the third Josephson Junction and the fourth Josephson Junction, wherein the third terminal is electrically connected to the loop between the second Josephson Junction and the third Josephson Junction;

the method further comprising:

applying a second control current to the fourth terminal; and

adjusting the second control current to minimize a flux noise of the mSOT for a given applied magnetic field.

14. The method of claim 13, wherein to minimize the flux noise for the given applied magnetic field is accomplished by adjusting the second control current so that the current-flux response function is substantially equal to the maximum absolute value thereof.

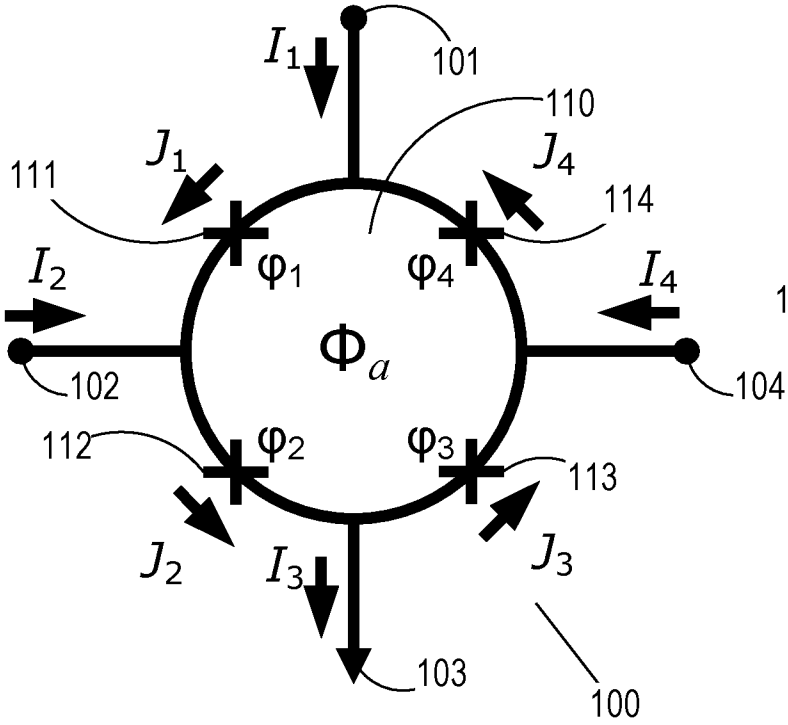


FIG. 1A

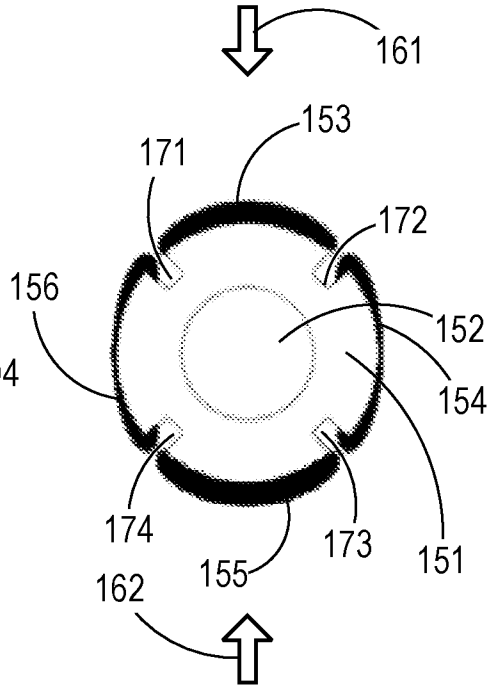


FIG. 1B

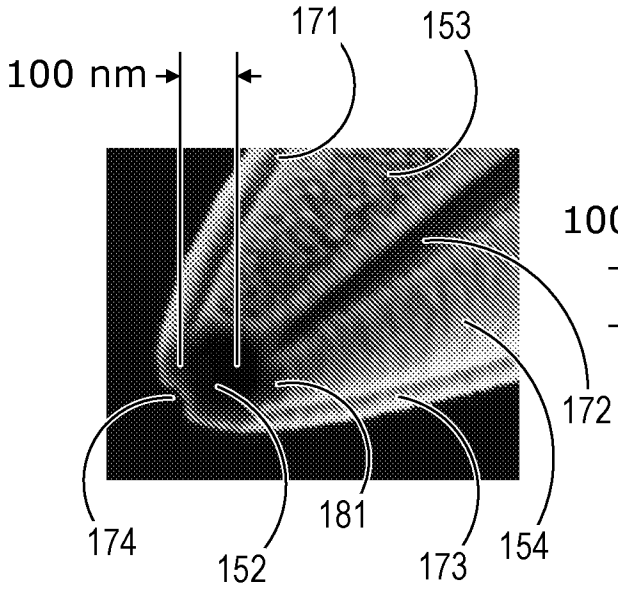


FIG. 1C

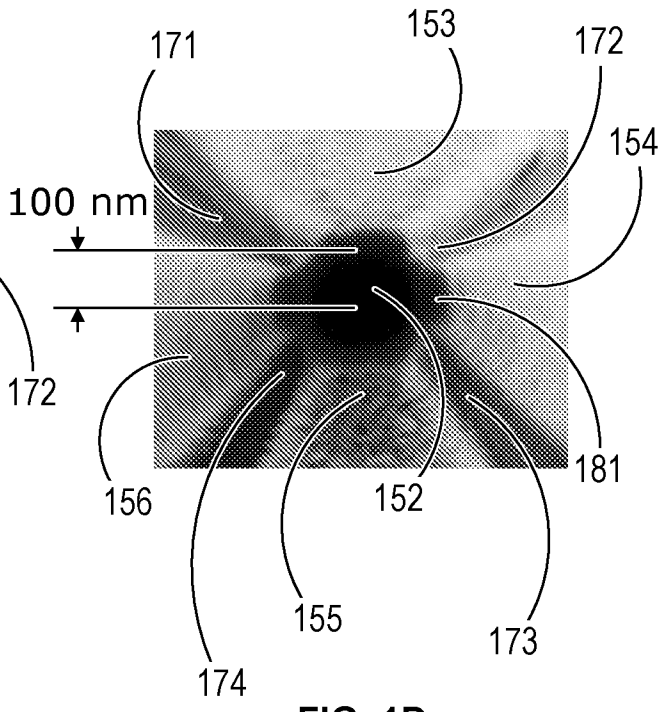


FIG. 1D

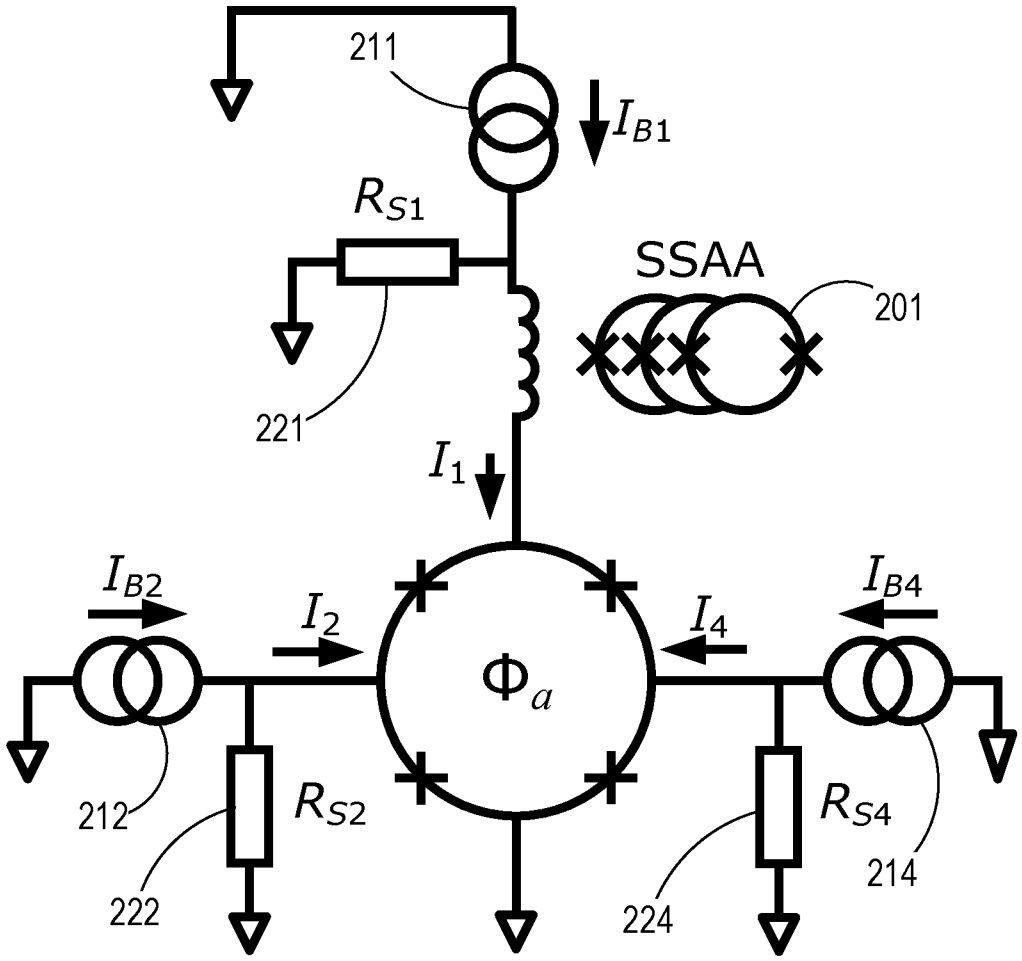

211
I_{B1}
R_{S1}
SSAA
201
221
I_1
I_{B2}
I_2
Φ_a
I_4
I_{B4}
212
R_{S2}
R_{S4}
214
222
224

FIG. 2A

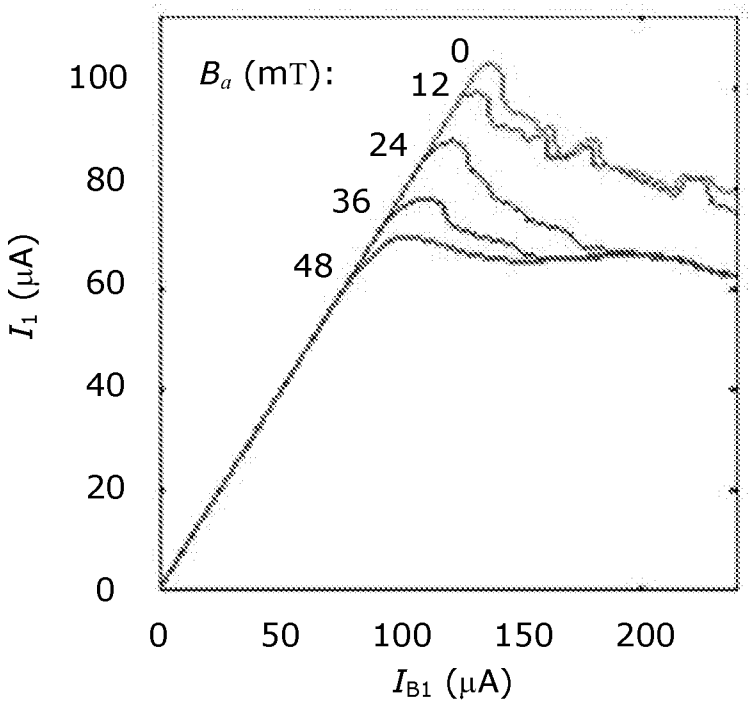

B_a (mT):
0
12
24
36
48
100
80
60
40
20
0
I_1 (μA)
0
50
100
150
200
I_{B1} (μA)

FIG. 2B

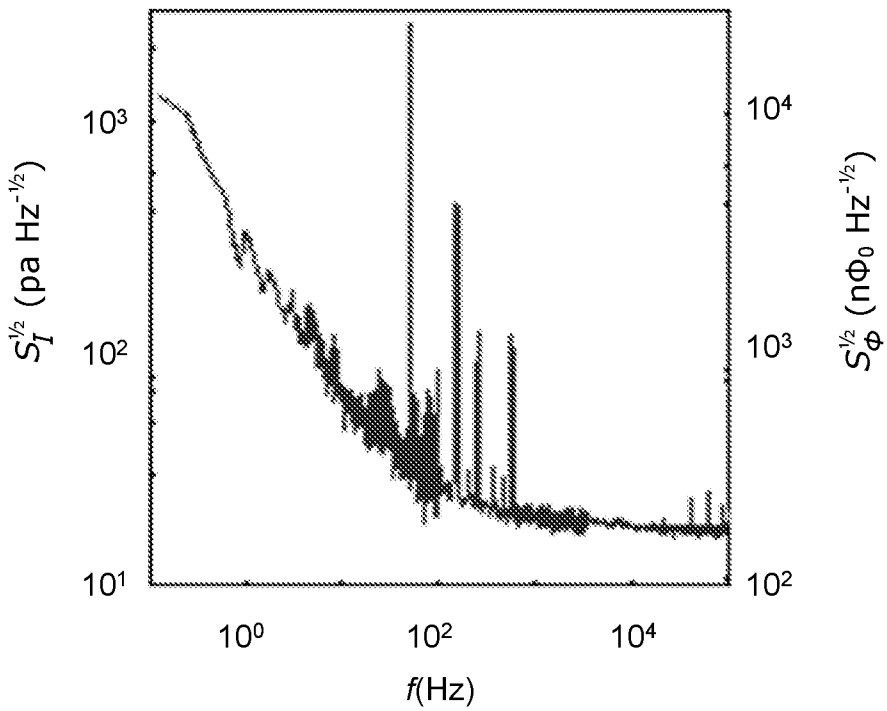

10^3
10^2
10^1
$S_I^{1/2}$ (pa Hz$^{-1/2}$)
10^4
10^3
10^2
$S_\Phi^{1/2}$ (nΦ$_0$ Hz$^{-1/2}$)
10^0
10^2
10^4
f(Hz)

FIG. 2C

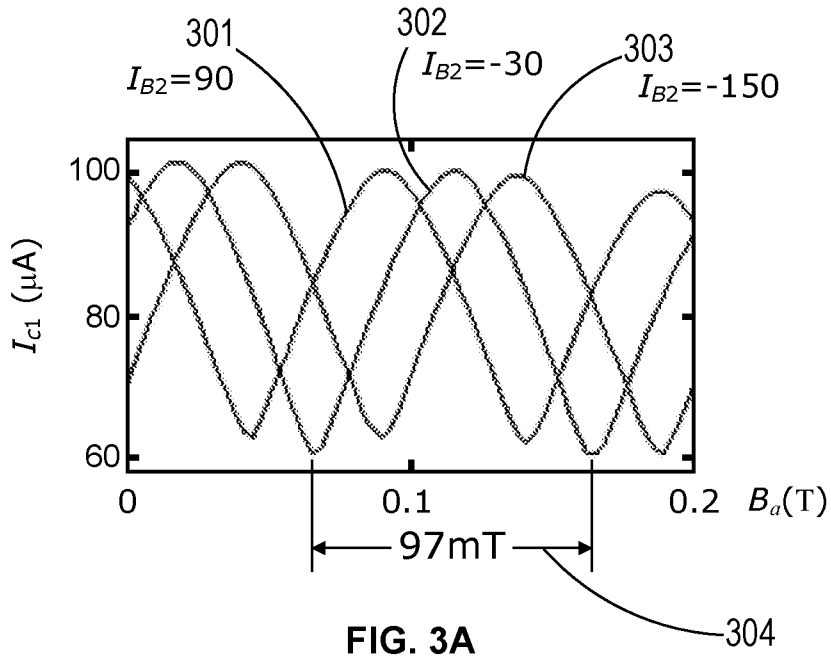

301
I_{B2}=90
302
I_{B2}=-30
303
I_{B2}=-150
100
80
60
I_{c1} (μA)
0
0.1
0.2
B_a(T)
97mT
304

FIG. 3A

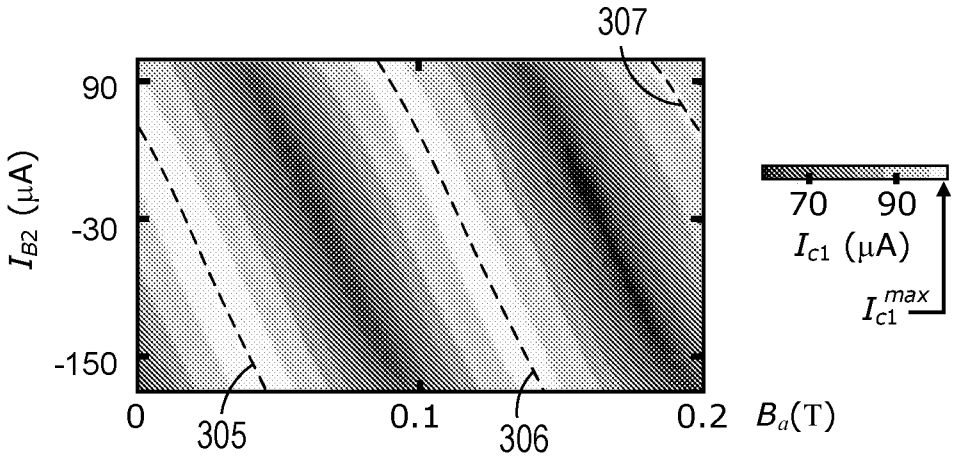

307
90
-30
-150
I_{B2} (μA)
0
0.1
0.2
B_a(T)
305
306
70
90
I_{c1} (μA)
I_{c1}^{max}

FIG. 3B

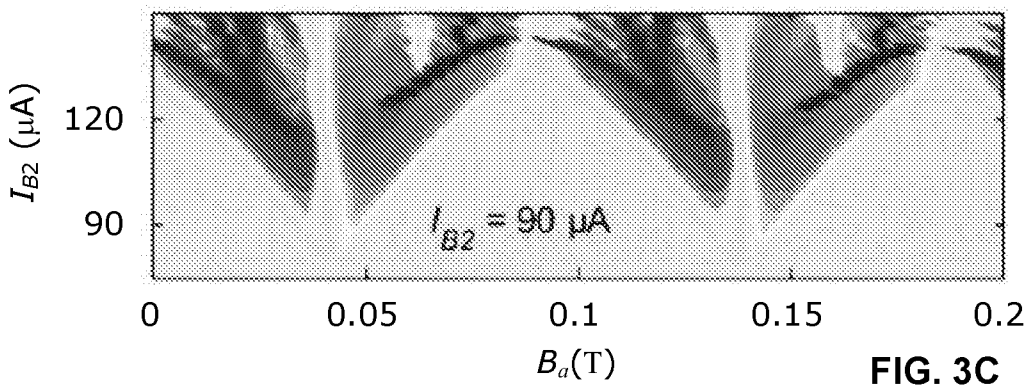


FIG. 3C

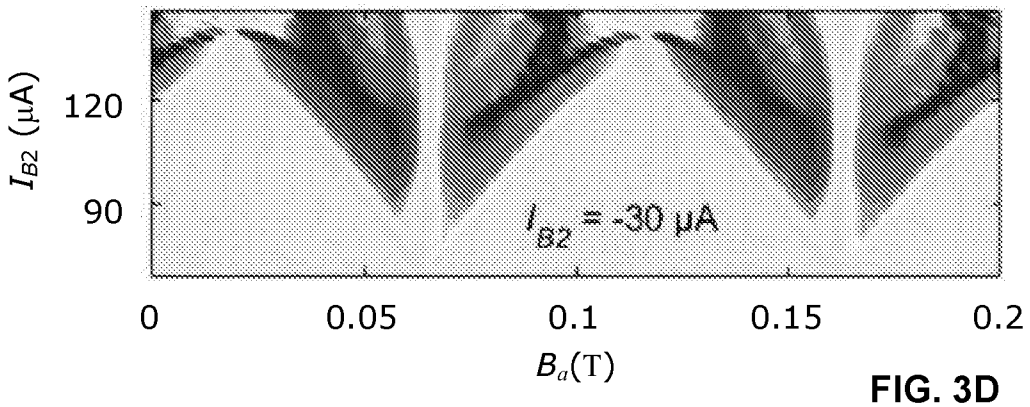


FIG. 3D

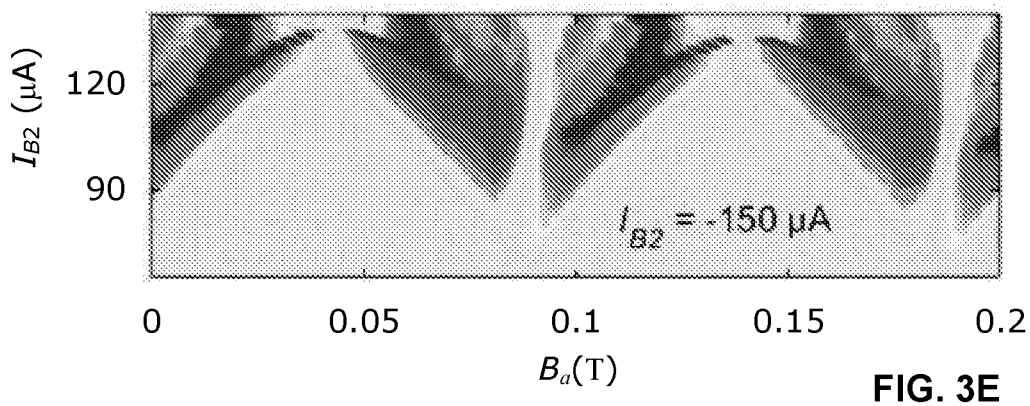


FIG. 3E



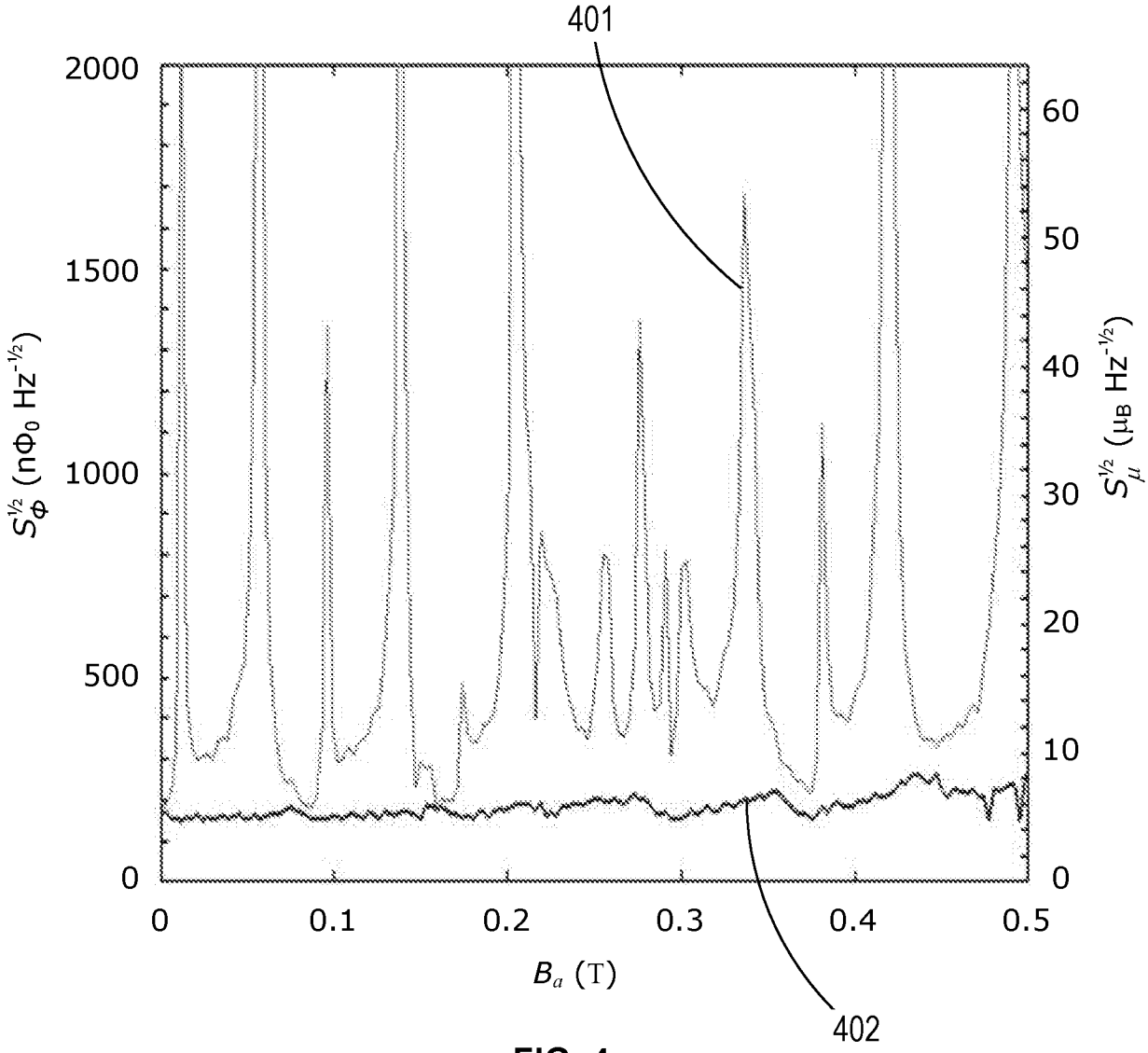
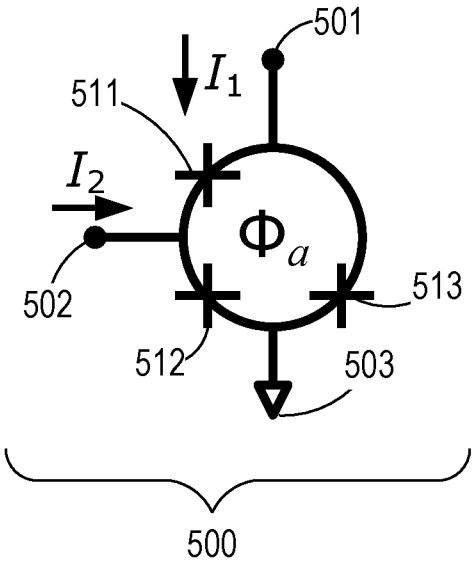

401
2000
1500
1000
500
0
60
50
40
30
20
10
0
0
0.1
0.2
0.3
0.4
0.5
B_a (T)
$S_\Phi^{1/2}$ ($n\Phi_0$ Hz$^{-1/2}$)
$S_\mu^{1/2}$ (μ_B Hz$^{-1/2}$)
402

FIG. 4


501
I_1
511
I_2
Φ_a
502
513
512
503
500

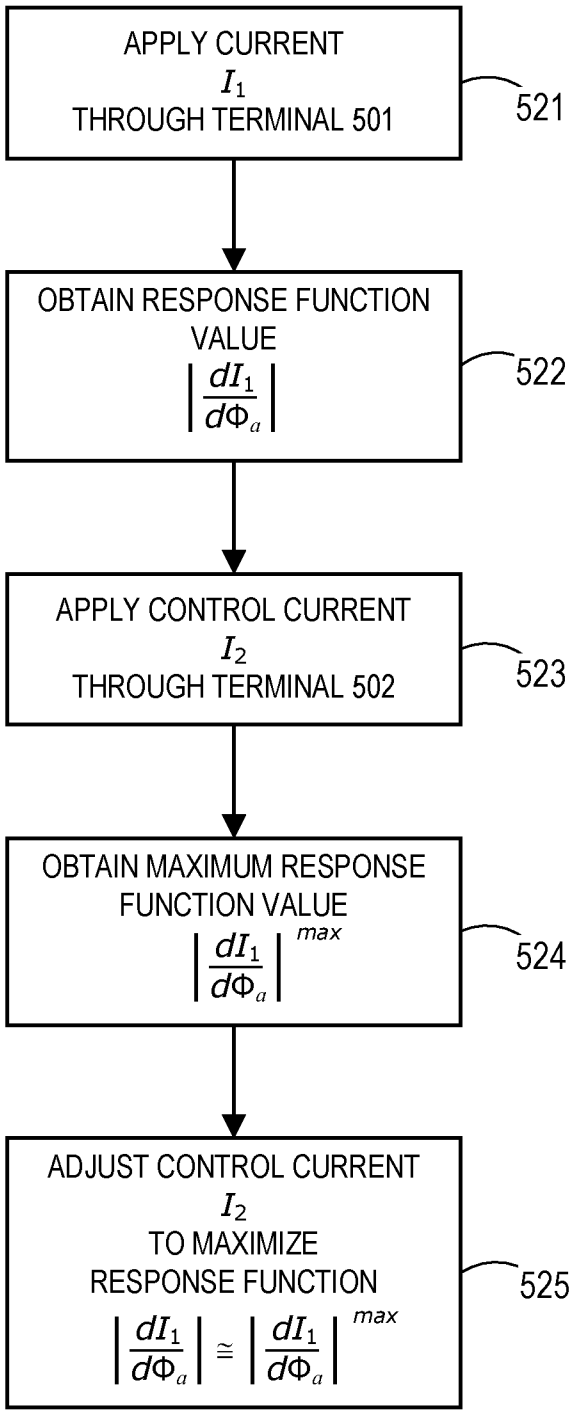
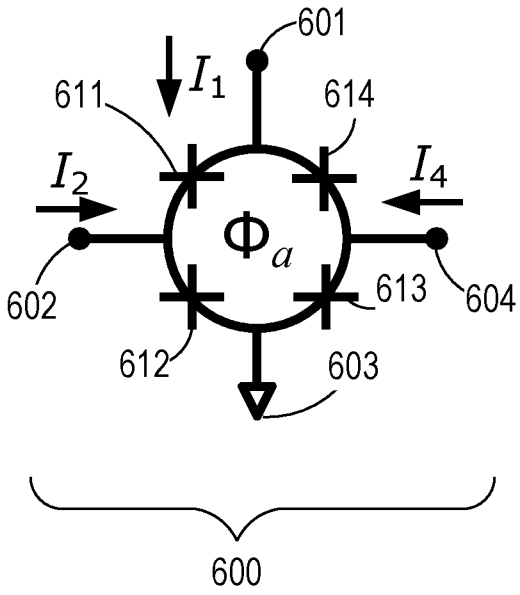

APPLY CURRENT I_1 THROUGH TERMINAL 501
521
OBTAIN RESPONSE FUNCTION VALUE $\left|\frac{dI_1}{d\Phi_a}\right|$
522
APPLY CONTROL CURRENT I_2 THROUGH TERMINAL 502
523
OBTAIN MAXIMUM RESPONSE FUNCTION VALUE $\left|\frac{dI_1}{d\Phi_a}\right|^{max}$
524
ADJUST CONTROL CURRENT I_2 TO MAXIMIZE RESPONSE FUNCTION $\left|\frac{dI_1}{d\Phi_a}\right| \cong \left|\frac{dI_1}{d\Phi_a}\right|^{max}$
525

FIG. 5


601
611
I_1
614
I_2
I_4
Φ_a
602
613
604
612
603
600

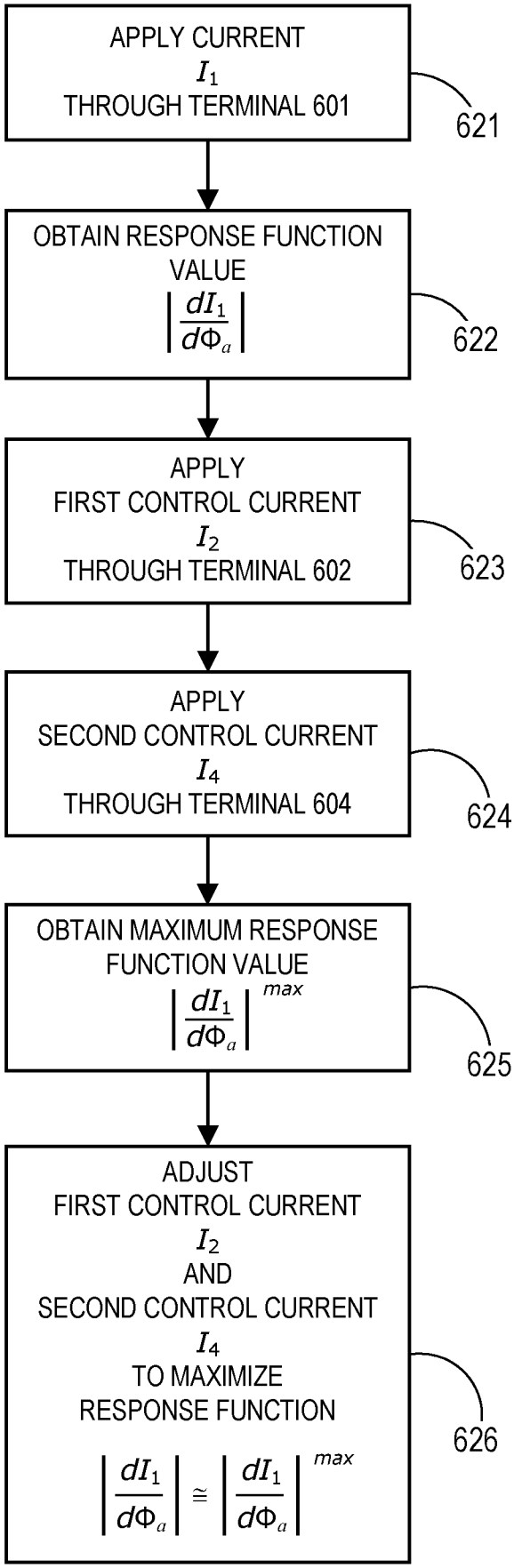

APPLY CURRENT I_1 THROUGH TERMINAL 601
621
OBTAIN RESPONSE FUNCTION VALUE $\left|\frac{dI_1}{d\Phi_a}\right|$
622
APPLY FIRST CONTROL CURRENT I_2 THROUGH TERMINAL 602
623
APPLY SECOND CONTROL CURRENT I_4 THROUGH TERMINAL 604
624
OBTAIN MAXIMUM RESPONSE FUNCTION VALUE $\left|\frac{dI_1}{d\Phi_a}\right|^{max}$
625
ADJUST FIRST CONTROL CURRENT I_2 AND SECOND CONTROL CURRENT I_4 TO MAXIMIZE RESPONSE FUNCTION $\left|\frac{dI_1}{d\Phi_a}\right| \cong \left|\frac{dI_1}{d\Phi_a}\right|^{max}$
626

FIG. 6

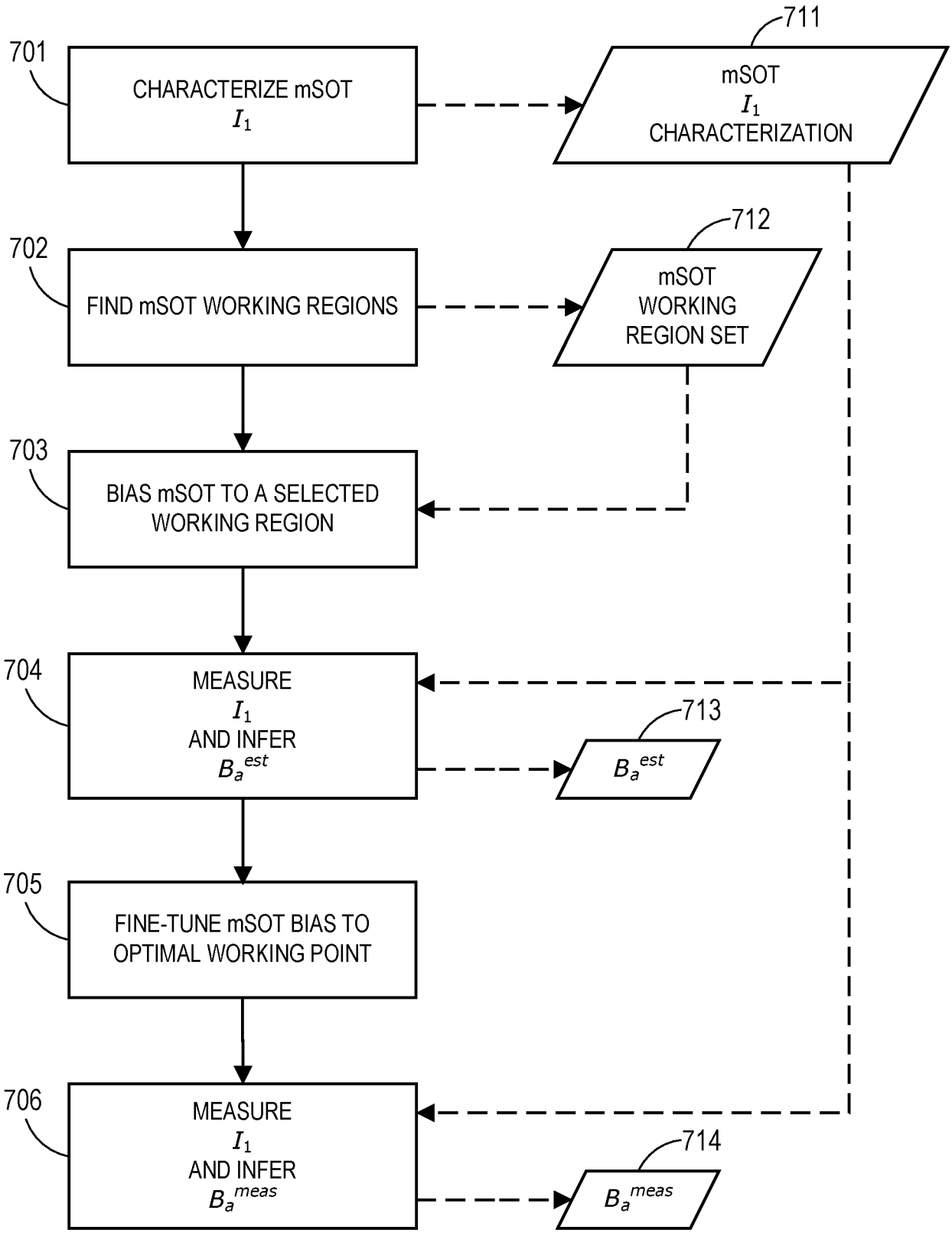

701
CHARACTERIZE mSOT
I_1
711
mSOT
I_1
CHARACTERIZATION
702
FIND mSOT WORKING REGIONS
712
mSOT
WORKING
REGION SET
703
BIAS mSOT TO A SELECTED
WORKING REGION
704
MEASURE
I_1
AND INFER
B_a^{est}
713
B_a^{est}
705
FINE-TUNE mSOT BIAS TO
OPTIMAL WORKING POINT
706
MEASURE
I_1
AND INFER
B_a^{meas}
714
B_a^{meas}

FIG. 7

INTERNATIONAL SEARCH REPORT

International application No.
PCT/IL2016/050421

A. CLASSIFICATION OF SUBJECT MATTER
IPC (2016.01) G01R 33/00, G01R 33/02, H01L 39/22, H01L 39/14

According to International Patent Classification (IPC) or to both national classification and IPC

B. FIELDS SEARCHED

Minimum documentation searched (classification system followed by classification symbols)
IPC (2016.01) H01L 39/22, H01L 39/14

Documentation searched other than minimum documentation to the extent that such documents are included in the fields searched

Electronic data base consulted during the international search (name of data base and, where practicable, search terms used)
Databases consulted: Esp@cenet, Google Patents, Google Scholar
Search terms used: Eli Zeldov, Y10S505/702/ Y10S505/861 as the Cooperative Patent Classification, multi channel multi junction, josephson junction

C. DOCUMENTS CONSIDERED TO BE RELEVANT

Category*	Citation of document, with indication, where appropriate, of the relevant passages	Relevant to claim No.
A	WO 2014188416 A1 REINER et al. 27 Nov 2014 (2014/11/27) the whole document	1-14
A	Three-Junction SQUID-on-Tip with Tunable In-Plane and Out-of-Plane Magnetic Field Sensitivity Nano Lett., 2014, 14 (11), pp 6481–6487 Publication Date (Web): October 13, 2014 Yonathan Anahory et al. 13 Oct 2014 (2014/10/13) the whole article	1-14
A	A scanning superconducting quantum interference device with single electron spin sensitivity Nature Nanotechnology 8, 639–644 (2013) doi:10.1038/nnano.2013.169 Denis Vasyukov et al. 01 Sep 2013 (2013/09/01) the whole article	1-14

[X] Further documents are listed in the continuation of Box C.

[X] See patent family annex.

* Special categories of cited documents:
"A" document defining the general state of the art which is not considered to be of particular relevance
"E" earlier application or patent but published on or after the international filing date
"L" document which may throw doubts on priority claim(s) or which is cited to establish the publication date of another citation or other special reason (as specified)
"O" document referring to an oral disclosure, use, exhibition or other means
"P" document published prior to the international filing date but later than the priority date claimed

"T" later document published after the international filing date or priority date and not in conflict with the application but cited to understand the principle or theory underlying the invention
"X" document of particular relevance; the claimed invention cannot be considered novel or cannot be considered to involve an inventive step when the document is taken alone
"Y" document of particular relevance; the claimed invention cannot be considered to involve an inventive step when the document is combined with one or more other such documents, such combination being obvious to a person skilled in the art
"&" document member of the same patent family

Date of the actual completion of the international search	Date of mailing of the international search report
01 Aug 2016	07 Aug 2016
Name and mailing address of the ISA: Israel Patent Office Technology Park, Bldg.5, Malcha, Jerusalem, 9695101, Israel Facsimile No. 972-2-5651616	Authorized officer Al-Muhannad Rafa Telephone No. 972-2-5651751

INTERNATIONAL SEARCH REPORT

International application No.
PCT/IL2016/050421

C (Continuation). DOCUMENTS CONSIDERED TO BE RELEVANT

Category*	Citation of document, with indication, where appropriate, of the relevant passages	Relevant to claim No.
A	Why NanoSQUIDs are important: an introduction to the focus issue Superconductor Science and Technology, Volume 22, Number 6 C P Foley1 and H Hilgenkamp2 14 May 2009 (2009/05/14) the whole article	1-14
A	US 5326986 A Miller JR John et al. 05 Jul 1994 (1994/07/05) the whole document	1-14

INTERNATIONAL SEARCH REPORT
Information on patent family members

International application No.
PCT/IL2016/050421

Patent document cited search report	Publication date	Patent family member(s)	Publication Date
WO 2014188416 A1	27 Nov 2014	WO 2014188416 A1	27 Nov 2014
		EP 2999972 A1	30 Mar 2016
		US 2016103192 A1	14 Apr 2016
US 5326986 A	05 Jul 1994	US 5326986 A	05 Jul 1994